LAWRENCE
LIVERMORE
NATIONAL
LABORATORY

LLNL-CONF-688397

Identification of solid materials using HSI spectral oscillators

C. L. Lanker, M. O. Smith

April 11, 2016

SPIE Defense + Security 2016
Baltimore, MD, United States
April 17, 2016 through April 21, 2016

Disclaimer

Identification of solid materials using HSI spectral oscillators

Cory L. Lanker[a] and Milton O. Smith[a]

[a]Lawrence Livermore National Laboratory, 7000 East Ave, Livermore, CA 94550

ABSTRACT

Our research aims to characterize solid materials through LWIR reflectance spectra in order to improve compositional exploitation in a hyperspectral imaging (HSI) sensor data cube. Specifically, we aim to reduce false alarm rates when identifying target materials without compromising sensitivity. We employ dispersive analysis to extract the material oscillator resonances from reflectance spectra with a stepwise fitting algorithm to estimate the Lorentz or Gaussian oscillators effectively present in the HSI spectral measurements. The proposed algorithm operates through nonlinear least squares minimization through a grid search over potential oscillator resonance frequencies and widths. Experimental validation of the algorithm is performed with published values of crystalline and amorphous materials. Our aim is to use the derived oscillator parameters to characterize the materials that are present in an HSI pixel. We demonstrate that there are material-specific properties of oscillators that show subtle variability when considering changes in morphology or measurement conditions. The experimentally verified results include variability in material particle size, measurement angle, and atmospheric conditions for six mineral measurements. Once a target material's oscillators are characterized, we apply statistical learning techniques to form a classifier based on the estimated spectral oscillators of the HSI pixels. We show that this approach has good initial identification results that are extendible across localized experimental conditions.

Keywords: hyperspectral, target detection, material composition, Gaussian basis functions, Lorentz oscillators, exploitation, inverse problem, pixel-scale model, curve-fitting

1. INTRODUCTION

This research aims to break away from the current exploitation paradigm that views a library of reflectance or emissivity spectra as the basis for material identification. Material identification techniques based on spectral libraries may have high false alarm rates in some field collect conditions while using an appropriate detection threshold.[1] We aim to improve field collect pixel-scale detection of target solids of an hyperspectral imaging (HSI) data cube using a supplemental alternative characterization of the reflectance spectra. Our approach is similar to the work of Brown[2] that links dips in absorption bands from HSI spectroscopy to material composition by the center wavelengths, widths, and amplitudes of spectral oscillators via curve-fitting.

The first of two problems we address is how to alternatively characterize reflectance using Lorentz oscillation theory or Gaussian basis functions using an automated routine that both fits a variety of spectra and is robust to noise. We show a physical basis for modeling reflectance using Lorentz oscillators and then use this model to justify a similar recharacterization using Gaussian basis functions. Our approach results in a stepwise algorithm that fits a collection of either Lorentz oscillators or Gaussian basic functions to a pixel's reflectance spectrum. These pixel-scale Lorentz and Gaussian profiles contain information necessary to reconstruct the signal-related part of the reflectance spectra helpful in characterizing the material in a pixel.

The second problem we address is how to use these Lorentz and Gaussian profiles for improved quantification of a pixel's material composition. We demonstrate that there are differences in these fit parameters across materials and that these same differences commonly occur across measurement conditions. Our approach results in a set of features—derived from the Lorentz or Gaussian parameters—that may be predictive in addressing material composition. We demonstrate that these Lorentz and Gaussian features are relatively insensitive to variable conditions experienced in HSI data collection and therefore contain additional information relevant to

Further author information: (Send correspondence to C.L.L.)
C.L.L.: E-mail: lanker1@llnl.gov, Telephone: 1 925 423 3583
M.O.S.: E-mail: smith428@llnl.gov

HSI exploitation. Our conclusion is that this alternative characterization of reflectance spectra can improve composition quantification of solid materials across atmospheric conditions, measurement angle, morphology, and composition.

Section 2 presents the fitting methods for Lorentz and Gaussian characterization and explains the LWIR data collection performed at Lawrence Livermore National Laboratory (LLNL) in 2015 that produced the HSI data used in this paper. Section 3 gives the results for exploitation with these spectral features derived from the fitting methods. A discussion in Section 4 concludes the paper.

2. ALTERNATE SPECTRAL CHARACTERIZATION OF HSI DATA

We propose an alternative characterization of the reflectance using basis functions derived from Lorentz oscillators or Gaussian density kernels. We want to transition from looking at magnitude of reflectance or emissivity and instead think of a characterization based on effective material-related oscillations. This alternative characterization of reflectance spectra will yield variables that are less dependent on background or atmospheric conditions than current exploitation methods. These variables derived from local reflectance features may be useful in quantifying material composition.

2.1 Lorentz Oscillator Characterization

The motivation for using Lorentz oscillations as a reflectance characterization method is the recovery of physics-related phenomena of solid materials. Lorentz oscillators for a material exhibit common structure across particle size and measurement conditions. This property leads us to believe that the Lorentz oscillator discovery process uncovers material-based properties. These pixel-derived oscillators may indicate more information about the presence of a target material from the formed reflectance spectrum.

Assume we have an HSI sensor-observed pixel reflectance with p bands, $R(\omega_i)$, $i = 1, \ldots, p$. We find the optimal K Lorentz oscillators with resonance frequency ω_0, line width γ, and strength A that reduce the squared errors $\sum_{i=1}^{p}(R(\omega_i)-\hat{R}(\omega_i))^2$, where is $\hat{R}(\omega)$ is the fit reflectance derived from K Lorentz oscillators. The dielectric function is calculated from the $3K+1$ Lorentz parameters $\epsilon(\omega) = \epsilon_\infty + \sum_{j=1}^{K} A_j\omega_{0j}^2/(\omega_{0j}^2 - \omega^2 - i\gamma_j\omega\omega_{0j})$, where ϵ_∞ is a constant term requiring estimation,[3] multiplying by the resonance frequency so the constants A_j and γ_j do not depend on frequency.[4] The fit reflectance is calculated from the dielectric $\hat{R}(\omega) = \left|\left(1 - \sqrt{\epsilon(\omega)}\right)/\left(1 + \sqrt{\epsilon(\omega)}\right)\right|^2$ using Frensel's equation.[4] Our algorithm determines K by assessing when further reduction of unexplained variation no longer justifies an additional Lorentz oscillator using three parameters. See Figure 1 for the dielectric constant and reflectivity functions for example Lorentz oscillators in the LWIR region based on those found in minerals.[5]

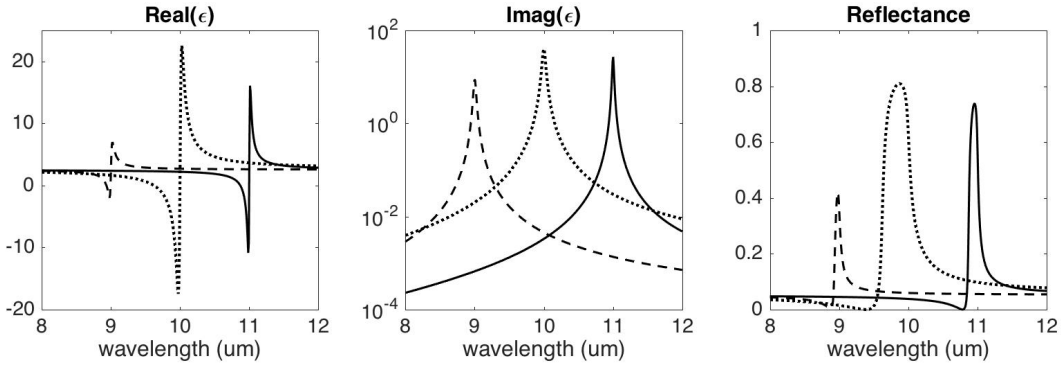

Figure 1. Example of three Lorentz oscillators plotted in dielectric constant and reflectivity using Frensel. The three oscillators are centered at 9, 10, and 11 um, with respective strength A of 0.05, 0.20, and 0.05, and line width γ of 0.005, 0.005, and 0.002. The term $\epsilon_\infty = 2.5$ for all plots.

By using a limited number of oscillators we can account for a large percentage of the variation of the reflectance spectra—typically 12 to 18 oscillators will account for over 98% of the spectral variability about its mean value

in terms of squared error. The algorithm stops adding oscillators when the reduction in sum of squared error is statistically too small to justify the three additional parameters for another Lorentz oscillator. As each Lorentz oscillation is characterized by its resonance frequency from the material, the line width of the oscillator, and its strength or magnitude, we transition to thinking of a reflectance spectrum as a mixture of oscillators in a two-dimensional Lorentz space: K points in a $\mathbb{R}^2$ space defined by the Lorentz oscillator resonance frequency ω_0 and line width γ. In Section 3 we demonstrate that analyzing a pixel's reflectance spectrum by this Lorentz oscillator profile (combinations of resonance frequencies and oscillation line widths) is another way to reduce dimension of the reflectance information for the purpose of HSI exploitation. Line strength A is initially not considered as all included oscillators have significant strength to reduce the sum of squared errors enough for inclusion by the algorithm; however, future analyses should utilize this additional information in the magnitude parameter.

We compose a reflectance spectrum using forward-stepwise fitting of Lorentz oscillators in MATLAB via nonlinear least squares optimization with the Levenberg-Marquardt algorithm. See Figure 2 for an example of our implemented fitting procedure on three synthetic reflectance spectra generated for 200 bands between 8 and 13 μm. The three spectra are composed of 3, 6, and 10 oscillators, respectively from left to right, while the algorithm fits 3, 6, and 8 oscillators. Uncorrelated Gaussian noise is added to these synthetic spectra to mimic sensor and collection noise. The oscillator-fitting algorithm correctly finds the oscillators before stopping when fitting first two spectra of Figure 2; however, the algorithm fits only eight of ten Lorentz oscillators for the rightmost spectrum. The amount of unexplained variation is very low for the fits, leaving only 0.2%, 2.1%, and 0.9% of the total squared errors unexplained. Even though these reconstructed reflectance spectra closely match the original reflectance, there isn't a guarantee that the Lorentz oscillators themselves are identifiable using this method. This fact leads us to pursue the Gaussian density kernel basis function representation of the reflectance as explained in the next subsection.

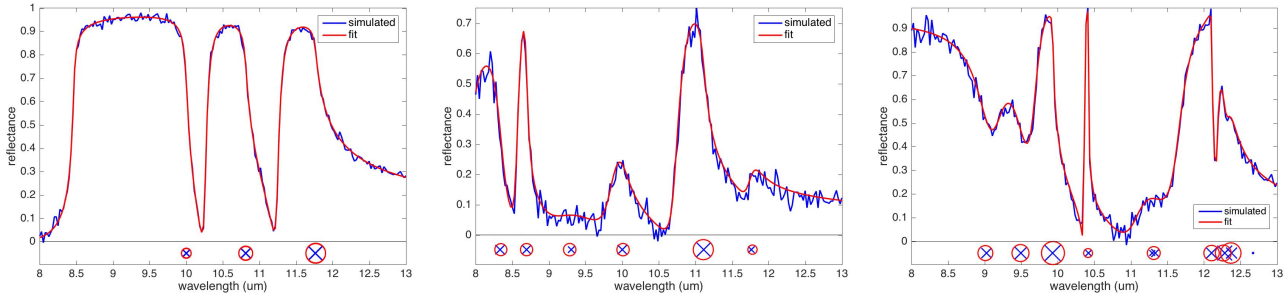

Figure 2. Examples of fitting simulated spectra (in blue) with resulting fitted reflectance (in red) using 3, 6, and 8 fit Lorentz oscillators, respectively. The wavelengths of the Lorentz oscillators in the synthetic spectra are shown by blue x's at bottom of plot, with size relative to amplitude parameter A. The fit oscillators are shown by red circles.

2.2 Gaussian Basis Function Characterization

We next transition to fitting reflectance spectra directly with basis functions from the bell-shaped density kernels of the Gaussian probability distribution. In rethinking material classification based on reflectance, we consider that the material fingerprint could exist directly in radiance or reflectance without the computationally-expensive fitting of Lorentz oscillators in the complex dielectric. We attempt to extract this fingerprint of local reflectance features by instead fitting Gaussian density kernels to the shape of the reflectance spectrum. These Gaussian basis function fits will supplement information in the assessment of material composition. By using a limited number of Gaussian basis functions, we can account for almost all of the variation in a pixel's reflectance spectra.

Each Gaussian density kernel composing the fit reflectance spectrum has three parameters: center wavelength, bandwidth, and magnitude. We compose the fitted reflectance $\hat{R}(\lambda)$ using Gaussian density kernels that minimizes the squared error for the p bands $\sum_{i=1}^{p}(R(\lambda) - \hat{R}(\lambda))^2$. The formula for a Gaussian density kernel with center wavelength μ, bandwidth σ (equivalently the Gaussian standard deviation), and magnitude c is $f(\lambda|\mu, \sigma, c) = c(\sqrt{2\pi}\sigma)^{-1} \exp(-(\lambda - \mu)^2/(2\sigma^2))$. The algorithm fits K Gaussian basis functions $f(\lambda|\mu, \sigma, c)$ until

further reduction in squared error is too small to justify another basis function and its three parameters, yielding fit reflectance $\hat{R}(\lambda) = \sum_{j=1}^{K} f(\lambda|\mu_j, \sigma_j, c_j)$.

These parameters are analogous to the three parameters of a Lorentz oscillator, and instead of characterization by resonance frequency and line width we now represent the mixture of Gaussian kernels in the two-dimensional space of center wavelength and bandwidth. Fitting basis functions derived from Gaussian kernels provides another way to characterize the information contained in reflectance spectra. See Figure 3 for the examples of Gaussian basis functions and how they relate to the reparameterized two-dimensional space (center wavelengths and bandwidths).

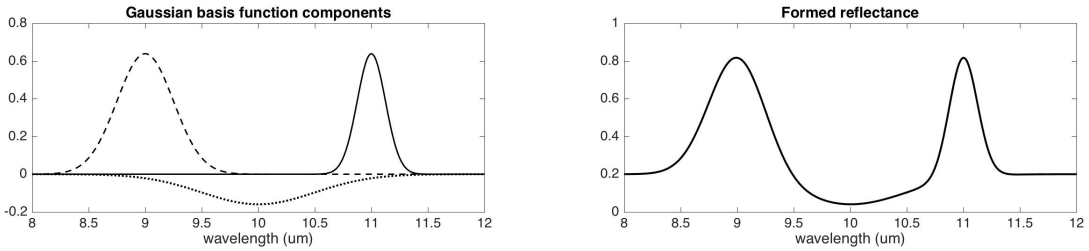

Figure 3. Examples of a reflectance spectrum formed with three Gaussian density kernel basis functions. The three curves on the left represent density kernels with center wavelengths μ at 9, 10, and 11um and bandwidths σ of 0.25, 0.5, and 0.125 um. Their respective magnitudes c are 0.5, -0.2, and 0.2. The curve on the right is the reflectance formed by the sum of these three Gaussian functions and a constant reflectance of 0.2.

The number of Gaussian basis functions required to sufficiently explain the reflectance curve is similar to the number of required Lorentz oscillators. In general, Gaussian basis functions can account for more of the reflectance variation, mainly because on average a few more Gaussian density kernels are fit to a spectrum. More basis functions are fit using the Gaussian representation rather than Lorentz oscillations because the fitting of Gaussians is done directly in the reflectance domain rather than fitting in the dielectric constant domain from which reflectance is calculated. See Figure 4 for an example of our implemented fitting procedure of Gaussian basis functions.

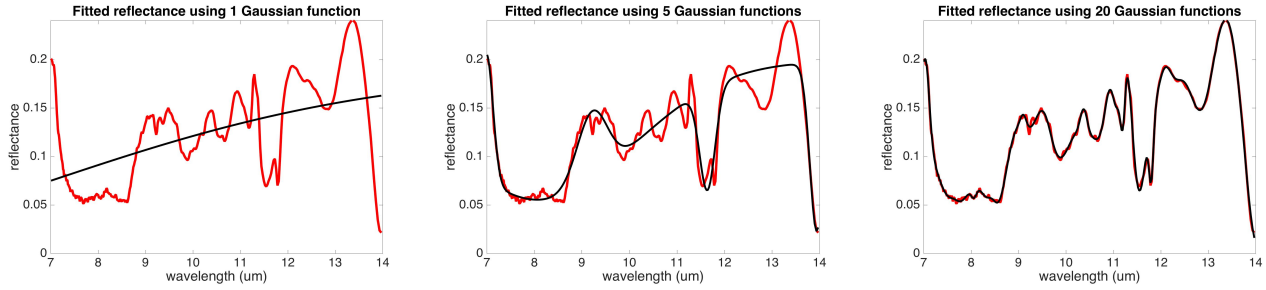

Figure 4. Example of forward stepwise fitting a reflectance spectrum with Gaussian basis functions (temporarily showing Lorentzians), using reflectance data of 90-125um calcite from Lane.[5]

2.3 Validation Data Sets

We will use diagnostics compared with Lorentz fits of the dishes of the LWIR spectral variation experiment performed at LLNL in 2015. The experiment measured seven minerals in petri dishes at various particle sizes, taking measurements at two difference view angles, during daytime and nighttime. We use the spectra from this collect under these various conditions to fit with Lorentz oscillators and Gaussian basis functions. The seven minerals are calcite, fused silica, jarosite, lepidolite, olivine, siderite, and talc. See Figure 5 for images of the collection setup. There are four different particle sizes for each mineral and the dish arrangement is scattered. The algorithms fit the reflectance spectra well for this experiment, see Figure 6 for the number of Gaussian basis functions fit per pixel and the resulting R^2 of the reflectance fit, where R^2 for the fitted reflectance $\hat{R}(\lambda)$ is $1 - \sum_\lambda (R(\lambda) - \hat{R}(\lambda))^2 / \sum_\lambda (R(\lambda) - \bar{R})^2$. We approach the use of the Lorentz and Gaussian fits in three steps. In each step, a 2-dimensional profile will be employed, as demonstrated in Figure 7.

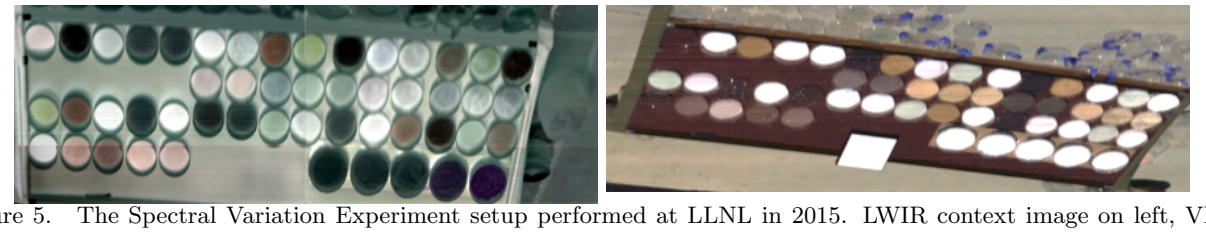

Figure 5. The Spectral Variation Experiment setup performed at LLNL in 2015. LWIR context image on left, VNIR context image on right.

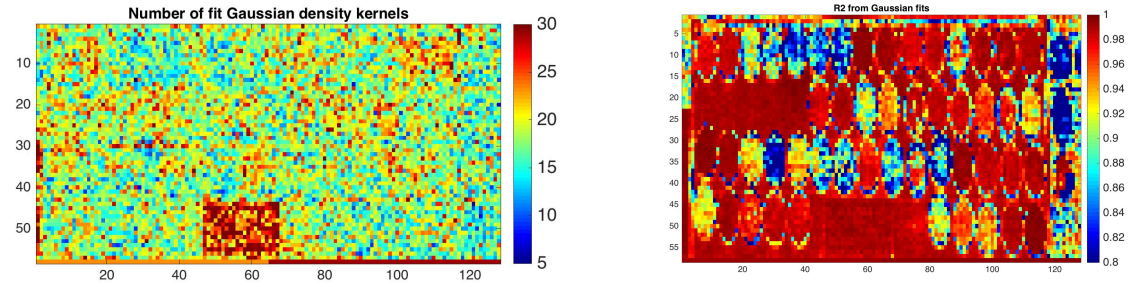

Figure 6. Quality of fits for the Spectral Variation Experiment. The number of Gaussian basis functions fit per pixel reflectance on left, the resulting statistical coefficient of determination R^2 for fit reflectance on right.

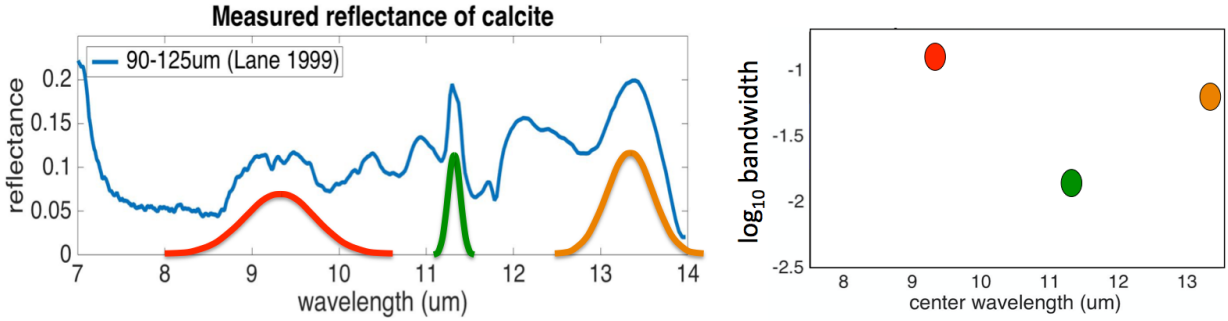

Figure 7. A profile showing locations on the 2-dimensional Gaussian parameter plane representing basis functions fit to the 90-125um calcite spectrum of Lane.[5] The plot on the right shows the locations in center wavelength μ and bandwidth σ (in log10) for three basis functions of the left plot, matched by color.

3. FEATURE CREATION FOR IMPROVED EXPLOITATION

We show that there are material-specific characteristics in the Lorentz or Gaussian two-dimensional parameter spaces previously defined that are useful for HSI exploitation, similar to the information in the reflectance itself using traditional exploit methods such as adaptive cosine estimator (ACE). This section presents positive results of using basic forms of these characteristics for material exploitation. Further, there are characteristics or features, i.e. particular combinations of Lorentz or Gaussian parameters, whose presence are highly indicative of a specific material. While a single feature will not indicate the presence of a specific material in the pixel because many materials may have the same feature, a certain combination of features may indicate the presence of the specific material as materials will exhibit different feature combinations across particle size and measurement condition.

First, we show that differences exist using the fitted Lorentz oscillator or Gaussian basis function parameters between target solid materials and all other materials. See Figure 8 for profile plots showing differences among the different materials for characterization with Lorentz oscillators and Gaussian basis functions, using data from the 2015 LLNL Spectral Variability Experiment. Differences between oscillators locations by material are apparent. Similar results are observed for 2-dimensional profiles derived from fit Gaussian basis functions.

Second, we test our hypothesis about the differences in Lorentz oscillator or Gaussian basis function profiles being useful for material identification. For testing, we learn about the Gaussian basis function locations in

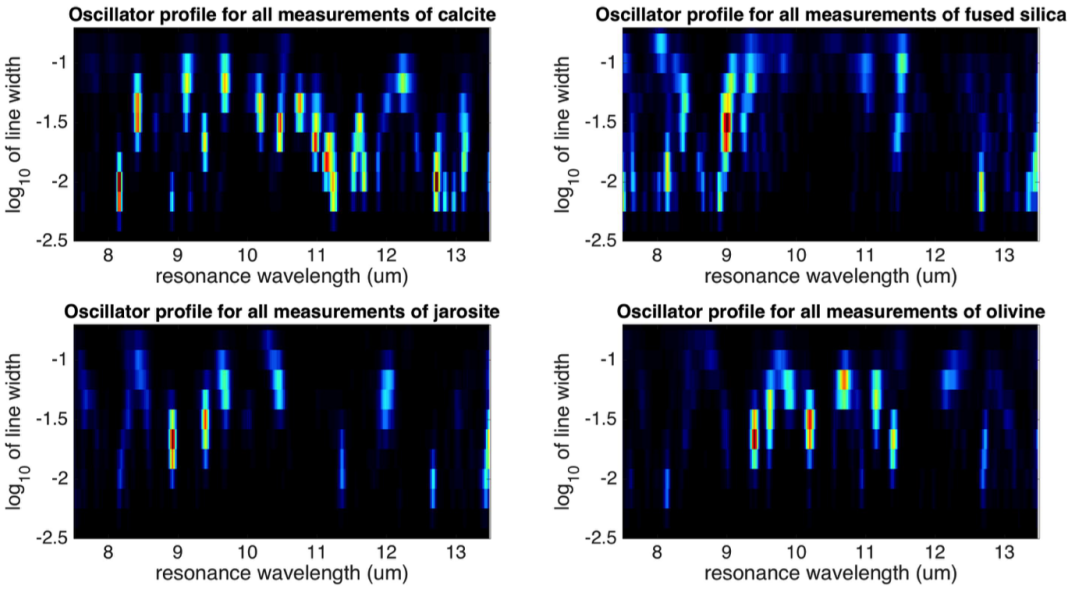

Figure 8. Differences between the hot spots of Lorentz oscillator 2-dimensional profiles showing logarithm of line width and resonance wavelength. Hot spots show where the fit oscillators are most concentrated for a given material. These plots aggregate the oscillators over all particle sizes and measurement conditions (nadir/off-angle, daytime/nighttime). Source: LLNL Spectral Variability Experiment.

the $(\lambda, \log_{10}\sigma)$ plane that are the most common for detecting calcite of the 45-63um particle size, which is the dish farthest at the top and right of Figures 5, 6, and 9, and only using the daytime observations, both nadir and off-angle (40 degrees). The scene used for testing the method are the nighttime observations at nadir. The goal of the analysis is to detect calcite, and the pixels we want to identify are in the center of the five calcite dishes. Any pixels in the outside of the calcite dishes are ignored for testing to prevent assigning a true positive as a false positive. We employ this cross-scene arrangement between training data and testing data to make the identification more difficult.

To do this material identification, we find the best oscillation locations (center frequency, bandwidth) that inform the presence of a target material and then simply compare a pixel's fit Gaussian basis function parameters to a target's profile as in Figure 8. See Figure 9 for a comparison of results using ACE compared with a method based on Gaussian fits. For ACE, the target spectrum is from the 45-63um particle size of calcite (all daytime observations), with the goal to ID all calcite particle sizes. The Gaussian method is able to detect all five calcite dishes in this nighttime at nadir scene. The Gaussian method can also detect a few pixels in the largest calcite particle size, while ACE completely misses that dish at location (25,18); this results in a higher ROC area under the curve for the Gaussian method.

4. DISCUSSION AND CONCLUSION

There are a few potential uses of this characterization method. The retrieved profiles associated with a material could be used as a filter mechanism—to remove clutter from a scene or provide a material-specific filtering. Anticipation of profile differences due to morphology or other changes that occur in the field could improve composition exploitation. It is the differences that appear in the field due to changes in atmosphere or clutter that affect identification and there may be information about material oscillations to limit this type of noise or field variability. This ability of extracting information from the reflectance—potentially complementary to the information that methods like ACE currently use—can be useful in identifying and detecting materials and thus to improve exploitation.

We have shown that it is possible to extract Lorentz oscillators and Gaussian basis functions for reconstruction of a reflectance spectrum. Our fitting algorithms use a forward stepwise curve-fitting approach using nonlinear

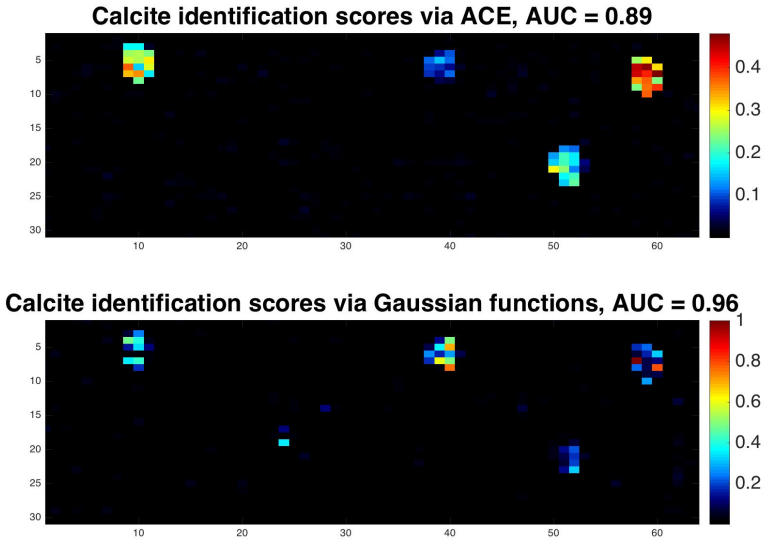

Figure 9. Identification task for calcite in the nighttime at nadir scene comparing results for ACE and a method derived from Gaussian features. ROC area under the curve is higher with the Gaussian method. The particle sizes from left to right are <45um, 125-250um, 90-125um, 63-90um, and 45-63um. Both methods are trained on spectra from the 45-63um calcite dish observed during daytime (observed at nadir and at off-angle). Data: Spectral Variation Experiment performed at LLNL in 2015.

least squares optimization. Using data from the 2015 LLNL Spectral Variability Experiment, material composition exploitation characterization of pixel reflectance spectra with these local features enhances exploitation of target solid materials. We aim to use the basis function fitting output to help characterize materials and answer the question if there is additional information in these profiles to assist exploitation. These methods can be advanced with a classification method from statistical learning techniques to determine the subset of predictors that are highly predictive of a certain material or to inform the features more useful to improving HSI exploitation.

ACKNOWLEDGMENTS

This work is performed under the auspices of the U.S. Department of Energy by Lawrence Livermore National Laboratory under Contract DE-AC52-07NA27344. The research described in this paper was supported by the U.S. Department of Energy National Nuclear Security Administration Office on Nonproliferation and Verification Research and Development.

REFERENCES

[1] Pieper, M. L., Manolakis, D., Lockwood, R., Cooley, T., Armstrong, P., and Jacobson, J., "Hyperspectral detection and discrimination using the ACE algorithm," in [*SPIE Optical Engineering + Applications*], **8158**, 807815, International Society for Optics and Photonics (2011).

[2] Brown, A. J., "Spectral curve fitting for automatic hyperspectral data analysis," *Geoscience and Remote Sensing, IEEE Transactions on* **44**(6), 1601–1608 (2006).

[3] Kuzmenko, A. B., "Kramers–Kronig constrained variational analysis of optical spectra," *Review of scientific instruments* **76**(8), 083108 (2005).

[4] Long, L., Querry, M., Bell, R., and Alexander, R., "Optical properties of calcite and gypsum in crystalline and powdered form in the infrared and far-infrared," *Infrared Physics* **34**(2), 191–201 (1993).

[5] Lane, M. D., "Midinfrared optical constants of calcite and their relationship to particle size effects in thermal emission spectra of granular calcite," *Journal of geophysical research* **104**(E6), 14099–14108 (1999).